A New Concept for Aircraft Dynamic Stability Testing

Martin E. Beyers*
National Research Council of Canada, Ottawa, Ontario, Canada

A new approach to dynamic stability testing is introduced, based on the concept of orbital fixed-plane motion. An apparatus is conceived with which an aircraft model is forced in an orbital path while constrained to the fixed-plane reference system. An exposition of the concept is given and the potential advantages in captive model testing and applications in flight mechanics are indicated. Using a single apparatus, it is possible to 1) determine a complete set of first-order, dynamic stability derivatives, 2) vary the relationships between the associated motion parameters, and 3) simulate modes of aircraft motion. A validation scheme, which exploits the considerable flexibility of the method, facilitates the extension of dynamic data to actual flight conditions.

Nomenclature

C_{ij} = dynamic stability derivative; $i = X, Y, Z, l, m, n$, $j = \dot{\alpha}, \dot{\beta}, q, r, \dot{\lambda}$
p, q, r = body axes angular velocities
r_0 = orbital radius
u, v, w = body axes velocity components
V = velocity
V_∞ = freestream velocity
x, y, z = body axes system
X, Y, Z = inertial frame of reference
x_c = center of mass coordinate
α = angle of attack $= \tan^{-1}(w/u)$
β = angle of sideslip $= \sin^{-1}(v/V)$
Γ = balance angle of pitch
Θ = strut pitch angle
$\dot{\lambda}$ = coning rate
Λ = tangential tilt angle
ξ, η, ζ = platform frame of reference
σ = orbital helix angle
Φ = orbital roll angle
ψ, θ, ϕ = modified Euler angles
Ψ = sting-shaft roll angle
ω = orbital angular velocity
Ω = reduced orbital frequency $= \omega r_0 / V_\infty$

Superscripts

$( )'$ = fixed-plane system
$(\hat{})$ = aerodynamic angles
$(\dot{})$ = differentiation with respect to time

Introduction

THE state-of-the-art of dynamic stability testing in wind tunnels has progressed significantly in recent years, in terms of the completeness of the set of dynamic derivatives which can be determined[1-3] as well as of the representativeness of motion conditions which can be simulated.[4,5] While these techniques can now provide much of the information required in aircraft flight simulation, there remains a need to further investigate the influence of experimental conditions on simulated dynamic characteristics and, in particular, on the dynamic stability derivatives in nonplanar motion at high angles of attack.

Consider, firstly, the determination of dynamic stability derivatives. The approach followed in the past has been based on oscillations of a captive (i.e., mechanically supported) model forced in one degree of freedom (DOF), termed the primary DOF. Apparatuses are available for the determination of dynamic cross and cross-coupling derivatives needed to describe rotary and translational motions[1-3] while the coning associated with aircraft nonplanar motion may be studied on rotary balances.[5] A complete set of derivatives required at least three apparatuses and five experiments. Now consider the experimental simulation of aircraft motion. For instance, steady spinning of an aircraft may be simulated on certain types of rotary balances. However, it has not been possible 1) to simulate the aircraft mode on the same apparatus used to determine the important lateral dynamic stability derivatives, and 2) to determine these derivatives under conditions of coning motion. The latter was pointed out by Orlik-Rückemann,[6] who noted that "... to study oscillatory spin, such as exhibited by many modern military aircraft, a combination of an oscillatory apparatus and a rotary balance would be required. Such a composite apparatus has not yet been constructed."

A new concept of captive-model dynamic stability testing embodying attribute 1 is introduced in this paper. It is shown to be possible, and practicable, to extract the full set of first-order dynamic derivatives and, in addition, to simulate representative aircraft motions, by means of a single apparatus. A more complete discussion of the approach may be found in the original report.[7]

While the motions produced by the proposed apparatus have one independent degree of freedom, the dynamic derivatives extracted have a 2DOF nature which might be exploited in several different ways. Although a specific type of mathematical model is suggested by the basic motions produced, it is not the purpose of this paper to deal with this subject; rather, the intention is to discuss the introduction of the new concept within the framework of the existing mathematical model of Tobak and Schiff.[8]

Concepts for Captive-Model Dynamic Testing

A concept of *orbital fixed-plane motion* is introduced in this paper. The term fixed-plane describes all motions of the aircraft model such that a transverse axis of the model is constrained to lie in a plane containing the horizontal Y and X axes of the inertial frame of reference. This body axes system is similar, although not identical to the fixed-plane coordinate system employed in missile flight dynamics.

Various special cases of fixed-plane motion, which can be generated mechanically, are considered here. These include the orbital fixed-plane modes for the determination of derivatives, fixed-plane coning, which represents a combination of characteristic motions, and several degenerate modes such as lunar coning and rolling.

Presented as Paper 81-0158 at the AIAA 19th Aerospace Sciences Meeting, St. Louis, Mo., Jan. 12-15, 1981; submitted Feb. 24, 1981; revision received March 8, 1982.

*Research Officer, Unsteady Aerodynamics Laboratory, National Aeronautical Establishment. Member AIAA.

Orbital Fixed-Plane Motion

Lateral Acceleration Derivatives

To visualize this new concept consider, at first, the simplest case, where the aircraft model is forced to translate along a circular path lying in a transverse plane while maintaining a fixed attitude as in Fig. 1a. Since the body angular velocities are zero and only the aerodynamic angles vary, this yields a pure lateral translational motion.

Rotational Derivatives

Now consider the case of pure angular motion. If the model is tilted through the helix angle while satisfying the fixed-plane constraint (see Fig. 1b), then the roll rate will be zero and the aerodynamic angles will be invariant, resulting in pure pitching and yawing motion.

Strictly speaking, these motions are not absolutely pure, being affected by small deflections of the sting under oscillatory aerodynamic loads and a constant inertial loading (which may be eliminated by an angular adjustment).

Note that the terms "orbital" and "fixed-plane" do not connote restrictions of the derivatives to be determined, nor are they descriptive of the aircraft motion being studied. Rather, they describe the motion of the sting/balance system; orbital motion is used in this case for the separation of rotational and translational motion parameters.

Fixed-Plane Coning

Now, if the model axis is tilted radially so that the center of mass lies on the orbital axis, then the model will describe a coning motion while subject to the fixed-plane constraint. The resulting motion is a combination of oscillatory pitching and yawing with steady coning at a common frequency when the axis is aligned with the wind vector.

General Arrangement of the Apparatus

The construction of a compact mechanical system having the physical characteristics required to generate all three fixed-plane modes for an aircraft model in a wind tunnel is perfectly feasible. The geometric features of such a system are illustrated in Fig. 2. There are two nonintersecting axes providing continuous rotations Φ and Ψ, which may be mutually inclined through a tilt angle Λ, and two additional, pivotal axes. The latter provide for the inclination Θ of the complete motion relative to the flow direction and of the model relative to the Ψ axis, through the angle Γ. The Φ and Ψ axes are respectively referred to as the orbital and sting axes. Therefore, the model and balance are mounted on a shaft, denoted the countershaft, rotating within the sting, which in turn rotates about the orbital axis. Note that the model center of mass must lie on the sting axis. Linear adjustments of the tilt axis and the radius of the orbital motion, r_0, are made in the plane of a rotating platform shown in Fig. 2.

To assist the reader in visualizing the motions described, the model depicted in Fig. 3 was constructed. A horizontal inclination, fixed orbital radius, and counterweight (which, of course, does not appear in the actual system) are used for simplicity.

Captive Fixed-Plane Motion

A captive model is constrained to a constant roll angle relative to the fixed-plane coordinate system, the orientation of which can be described at all times by two successive Euler rotations. Explicit relationships for the motion variables[7] can be obtained by performing transformations with reference to the inertial (X,Y,Z), fixed-plane (x',y',z') and body (x,y,z) axes systems and an auxiliary "platform" frame of reference (ξ,η,ζ) as depicted in Fig. 4. The orbital axis is inclined at an angle Θ with respect to the X axis in the vertical X-Z plane. The platform frame is parallel to the inertial system and translates in a circular path which is the hodograph of the position vector r_0. The freestream velocity vector therefore

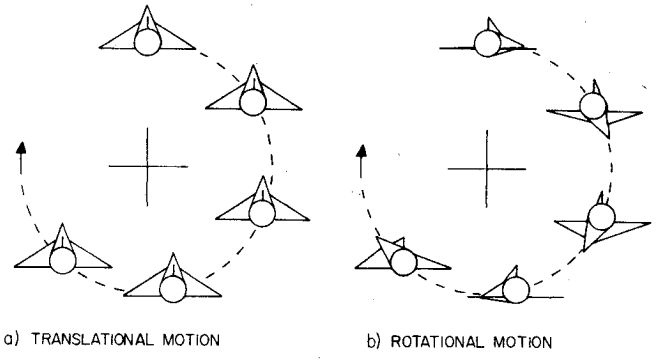

Fig. 1 Orbital fixed-plane motion.

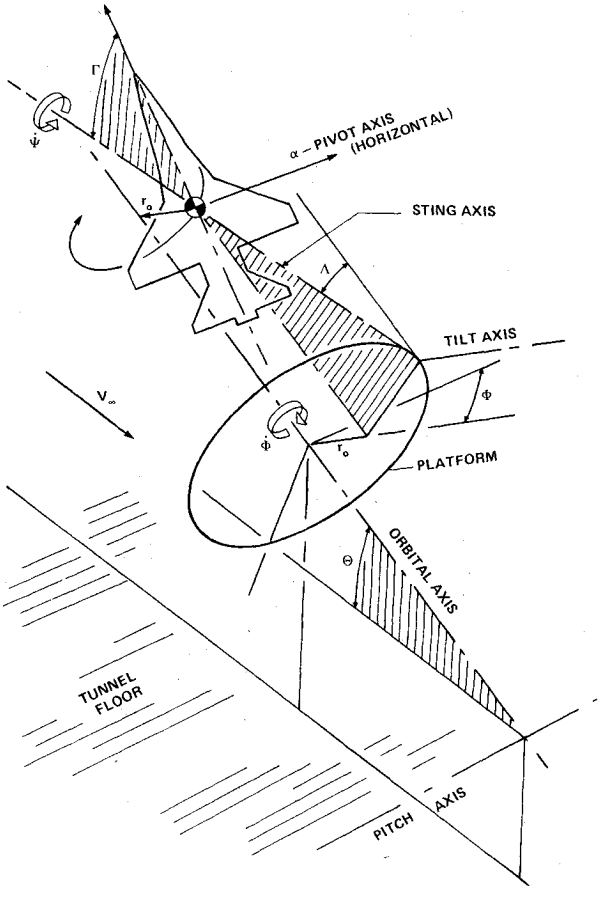

Fig. 2 Geometric arrangement of the apparatus.

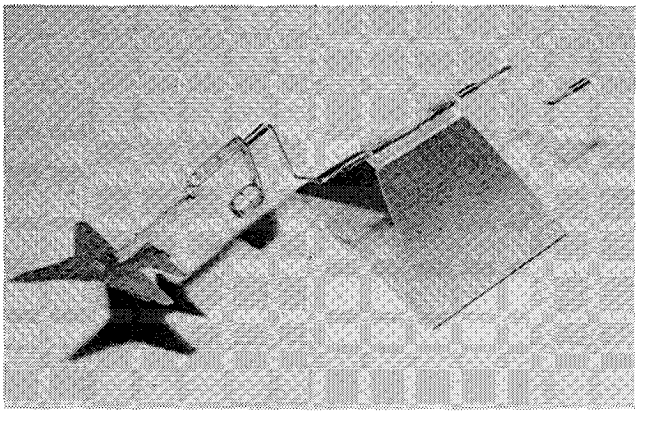

Fig. 3 Conceptual model of the orbital apparatus.

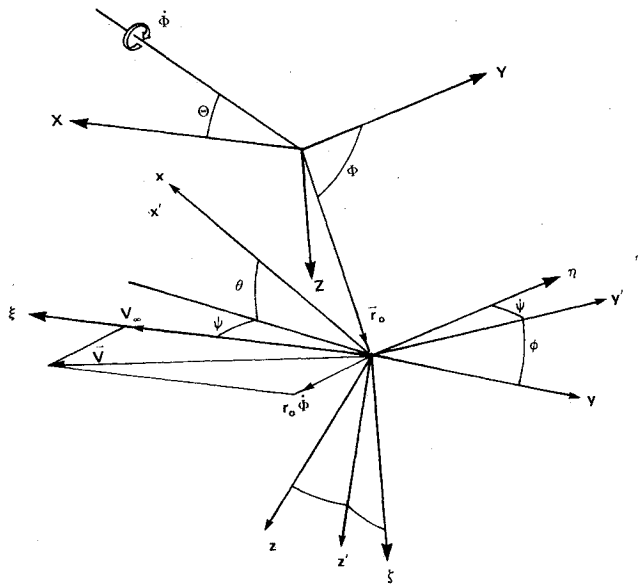

Fig. 4 Reference systems.

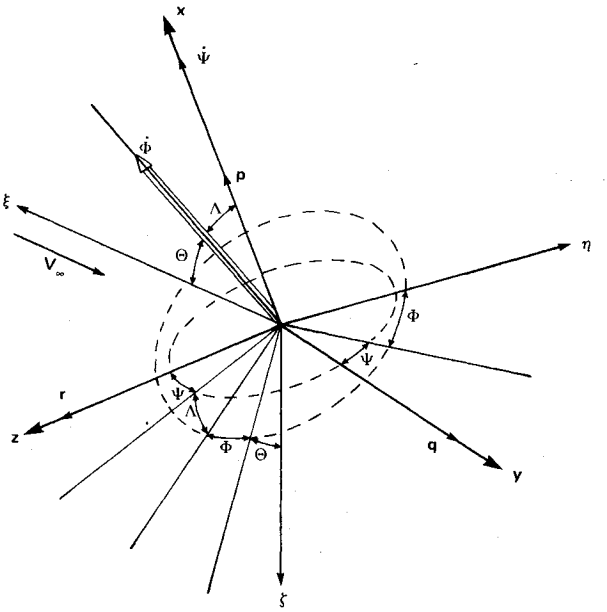

Fig. 5 Sequence of rotations (inclined axis).

remains aligned along the ξ axis while the spin axis is along x.

The position of the model is then determined by rotations through the angles Θ and Φ relative to the inertial frame and Λ, Ψ, and Γ relative to the platform system (see Fig. 2). Two cases will be considered. In the first the orbital axis is inclined at the pitch angle Θ with $\Gamma=0$, while in the second, the orbital axis is horizontal ($\Theta=0$) with the model pitched through an angle Γ relative to the Ψ axis.

Inclined Orbital Axis

The velocity due to orbital motion of a circular frequency $\omega=\dot{\Phi}$ is $\omega\times r_0$. Then, if (i,j,k) is a unit vector in the inertial system, the total velocity vector is

$$V=i(V_\infty+\omega r_0\cos\Phi\sin\Theta)-j\omega r_0\sin\Phi+k\omega r_0\cos\Phi\cos\Theta \quad (1)$$

and introducing the reduced orbital frequency $\Omega=\omega r_0/V_\infty$,

$$V=V_\infty(1+2\Omega\cos\Phi\sin\Theta+\Omega^2)^{1/2} \quad (2)$$

The sequence of rotations is Θ,Φ,Λ,Ψ; and the orbital and shaft angular velocities are $\dot{\Phi}$ and $\dot{\Psi}$, respectively, as shown in Fig. 5.

Pure Translational Motion ($\Lambda=0$)

To obtain translational motion of frequency ω at an angle of incidence Θ, the angular velocities are $\dot{\Psi}=-\dot{\Phi}=-\omega$ and $p=q=r=0$. The relationships for α and β and their derivatives follow from geometric considerations, for the combination of angles ψ, θ, and ϕ of interest. For instance, for the case $\psi=\phi=0$, $\theta=\Theta$ and the following results are obtained, using Eq. (2),

$$\beta=\sin^{-1}\{-\Omega\sin\Phi(1+2\Omega\cos\Phi\sin\Theta)^{-1/2}\}$$

$$\alpha=\tan^{-1}\{\tan\Theta+\Omega\cos\Phi/\cos\Theta\} \quad (3)$$

where the terms in Ω^2 have been neglected in comparison with unity, since Ω is of the order 0.02. Then, since $\dot{\beta}=(\dot{v}-v\dot{V}/V)/(V^2-v^2)^{1/2}$ and $\dot{\alpha}=(u\dot{w}-w\dot{u})/(u^2+w^2)$,

$$\dot{\beta}=-\omega\Omega\cos\Phi(1+2\Omega\cos\Phi\sin\Theta)^{-1/2}$$

$$\dot{\alpha}=-\omega\Omega\sin\Phi\cos\Theta/(1+2\Omega\cos\Phi\sin\Theta) \quad (4)$$

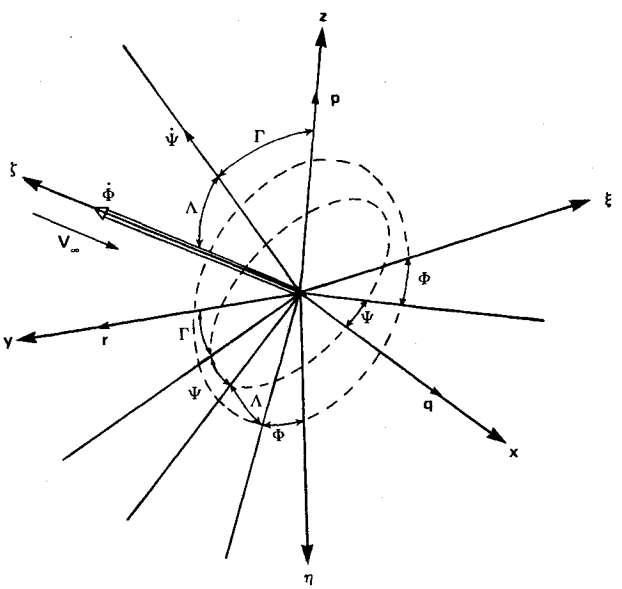

Fig. 6 Sequence of rotations (horizontal axis).

where terms in Ω^2 have again been neglected.

As Ω is small, the fluctuations in β, $\dot{\beta}$, and $\dot{\alpha}$ are essentially sinusoidal, while the α change is a true sinusoid. This form is also approached in β, $\dot{\alpha}$, and $\dot{\beta}$ as $\Theta\to 0$, while $\dot{\alpha}\to 0$ as $\Theta\to\pi/2$.

Pitching and Yawing

In this mode of operation $\dot{\Psi}=-\dot{\Phi}=-\omega$ as before, and since the roll rate of the fixed-plane system $p=-\dot{\psi}\sin\theta$ is small, the motion is essentially pitching and yawing. Note that this term is also present during yawing oscillations at nonzero pitch angles in conventional forced-oscillation experiments.

The velocity components transform as follows:

$$\begin{bmatrix} u \\ v \\ w \end{bmatrix} = [A_x] \begin{bmatrix} V_\infty+\omega r_0\cos\Phi\sin\Theta \\ -\omega r_0\sin\Phi \\ \omega r_0\cos\Phi\cos\Theta \end{bmatrix} \quad (5)$$

From Fig. 5 it is clear that to achieve fixed-plane motion, $\Psi = -\Phi$. Then the transformation matrix A_x representing the rotations through the angles Θ, Φ, Λ, and Ψ is

$$[A_x] = \begin{bmatrix} \cos\Lambda\cos\Theta - \sin\Lambda\cos\Phi\sin\Theta & \sin\Lambda\sin\Phi & -\cos\Lambda\sin\Theta - \sin\Lambda\cos\Phi\cos\Theta \\ -\sin\Lambda\sin\Phi\cos\Theta + \cos\Phi\sin\Phi\sin\Theta - \cos\Lambda\cos\Phi\sin\Phi\sin\Theta & \cos^2\Phi + \cos\Lambda\sin^2\Phi & \sin\Lambda\sin\Phi\sin\Theta + \cos\Phi\sin\Phi\cos\Theta - \cos\Lambda\sin\Phi\cos\Phi\cos\Theta \\ \sin\Lambda\cos\Phi\cos\Theta + \sin^2\Phi\sin\Theta + \cos\Lambda\cos^2\Phi\sin\Theta & \sin\Phi\cos\Phi - \cos\Lambda\cos\Phi\sin\Phi & -\sin\Lambda\cos\Phi\sin\Theta + \sin^2\Phi\cos\Theta + \cos\Lambda\cos^2\Phi\cos\Theta \end{bmatrix} \tag{6}$$

The tilt angle Λ will be set at values of the order of the orbital helix angle and is therefore necessarily small, 0[2 deg]. Therefore Eq. (5) may be written

$$\begin{bmatrix} u \\ v \\ w \end{bmatrix} = \begin{bmatrix} \cos\Theta - \Lambda\cos\Phi\sin\Theta & \Lambda\sin\Phi & -\sin\Theta - \Lambda\cos\Phi\cos\Theta \\ -\Lambda\sin\Phi\cos\Theta & 1 & \Lambda\sin\Phi\sin\Theta \\ \Lambda\cos\Phi\cos\Theta + \sin\Theta & 0 & \cos\Theta - \Lambda\cos\Phi\sin\Theta \end{bmatrix} \begin{bmatrix} V_\infty + \omega r_0\cos\Phi\sin\Theta \\ -\omega r_0\sin\Phi \\ \omega r_0\cos\Phi\cos\Theta \end{bmatrix} \tag{7}$$

Setting

$$\Lambda = -\omega r_0/(V_\infty\cos\Theta) = -\Omega/\cos\Theta \tag{8}$$

where $\Omega/\cos\Theta$ is the helix angle, and simplifying, the body axes velocity components are obtained from Eq. (7):

$$u = V_\infty(\cos\Theta + \Omega\cos\Phi\tan\Theta + \Omega^2/\cos\Theta)$$

$$v = 0 \qquad w = V_\infty\sin\Theta \tag{9}$$

Again, since Ω is small, the term in Ω^2 may be neglected. Then the aerodynamic angles and their derivatives are

$$\beta = 0 \qquad \dot{\beta} = 0$$

$$\alpha = \tan^{-1}\{\tan\Theta/(1 + \Omega\cos\Phi\tan\Theta\sec\Theta)\}$$

$$\dot{\alpha} = \omega\Omega\sin\Phi\sin^2\Theta\sec\Theta/(1 + 2\Omega\cos\Phi\sin\Theta) \tag{10}$$

Equations (9) and (10) are qualified only by the assumption of small reduced frequencies and hold for all Θ in the range $-\pi/2 \le \Theta \le \pi/2$ ($\beta = \dot{\beta} = 0$ for all Θ).

This is not a pure rotational motion since $\dot{\alpha}$ is nonzero. However, the linear acceleration component is significant only at large pitch angles, vanishing when $\Theta \to 0$. Comparing Eqs. (4) and (10) it is found that at $\Theta = 30$ deg this acceleration is exactly one-third of that generated in pure translation.

The magnitudes of the pitching and yawing angular velocities are usually much larger than their linear acceleration counterparts. Expressing the body axes rotational rates in terms of the sting position angles (see Fig. 5), assuming Λ is small, and using Eq. (8),

$$p = 0 \qquad q = \omega\Omega\sin\Phi/\cos\Theta \qquad r = -\omega\Omega\cos\Phi/\cos\Theta \tag{11}$$

From Eqs. (10) and (11),

$$\dot{\alpha} = q\sin^2\Theta/(1 + 2\Omega\cos\Phi\sin\Theta) \qquad q/r = -\tan\Phi \tag{12}$$

At $\Theta = 30$ deg, q exceeds $\dot{\alpha}$ by a factor greater than 4 so that for small to moderate pitch angles, the motion is effectively a pure pitching and yawing oscillation.

Horizontal Orbital Axis

The sequence of rotations in horizontal, orbital fixed-plane motion is Φ, Λ, Ψ, Γ, as illustrated in Fig. 6. The pertinent transformation matrix may be derived by setting $\Theta = 0$ in Eq. (7), followed by a rotation through Γ. Then

$$\begin{bmatrix} u \\ v \\ w \end{bmatrix} = \begin{bmatrix} \cos\Gamma - \Lambda\cos\Phi\sin\Gamma & \Lambda\sin\Phi\cos\Gamma & -\Lambda\cos\Phi\cos\Gamma - \sin\Gamma \\ -\Lambda\sin\Phi & 1 & 0 \\ \sin\Gamma + \Lambda\cos\Phi\cos\Gamma & \Lambda\sin\Phi\sin\Gamma & -\Lambda\cos\Phi\sin\Gamma + \cos\Gamma \end{bmatrix} \begin{bmatrix} V_\infty \\ -\omega r_0\sin\Phi \\ \omega r_0\cos\Phi \end{bmatrix} \tag{13}$$

Pure Rotational Motion

Setting $\Lambda = -\Omega$ as before, Eq. (13) yields

$$u = V_\infty\cos\Gamma(1 + \Omega^2) \qquad v = 0 \qquad w = V_\infty\sin\Gamma(1 + \Omega^2) \tag{14}$$

$$\alpha = \Gamma \qquad \beta = \dot{\beta} = \dot{\alpha} = 0 \tag{15}$$

where Ω^2 may be neglected. As is to be expected, Eqs. (9) and (10) reduce to this simple form when Θ and $\Gamma \to 0$.

Referring to Fig. 6, it is found that the body angular velocities transform as follows:

$$\begin{bmatrix} p \\ q \\ r \end{bmatrix} = \begin{bmatrix} \cos\Gamma & 0 & -\sin\Gamma \\ 0 & 1 & 0 \\ \sin\Gamma & 0 & \cos\Gamma \end{bmatrix} \begin{bmatrix} \dot{\Phi}\cos\Lambda - \dot{\Phi} \\ -\dot{\Phi}\sin\Lambda\sin\Phi \\ \dot{\Phi}\sin\Lambda\cos\Phi \end{bmatrix} \tag{16}$$

Using Eq. (8) and recalling that Λ is small,

$$p = \omega\Omega\cos\Phi\sin\Gamma$$

$$q = \omega\Omega\sin\Phi$$

$$r = -\omega\Omega\cos\Phi\cos\Gamma \tag{17}$$

This result agrees with Eq. (11) when $\Theta = \Gamma = 0$, as it should.

Pure Translational Motion

The rotational angular velocities are eliminated when $\Lambda = 0$. Then Eq. (13) yields

$$u = V_\infty\cos\Gamma - \omega r_0\cos\Phi\sin\Gamma$$

$$v = -\omega r_0\sin\Phi$$

$$w = V_\infty\sin\Gamma + \omega r_0\cos\Phi\cos\Gamma \tag{18}$$

whence, neglecting Ω^2 in comparison with unity,

$$\beta = \sin^{-1}\{-\Omega\sin\Phi\}$$

$$\alpha = \tan^{-1}\{(\tan\Gamma + \Omega\cos\Phi)/(1 - \Omega\cos\Phi\tan\Gamma)\} \tag{19}$$

$$\dot{\beta} = -\omega\Omega\cos\Phi \qquad \dot{\alpha} = -\omega\Omega\sin\Phi \tag{20}$$

These equations may be compared with Eqs. (3) and (4). While they reduce to the same result when $\Theta = \Gamma = 0$, the equations for a horizontal orbital axis have the advantage that $\dot{\beta}$ and $\dot{\alpha}$ are independent of the pitch angle. Moreover, as might have been deduced from geometric considerations, $\dot{\alpha}$ is of equal magnitude but different sense to the pitching velocity q obtained for $\Lambda = -\Omega$ [Eq. (17)], while a similar conclusion may be drawn for $\dot{\beta}$ on the one hand and the vector $r+p$ on the other.

General

It was considered desirable to check the transformation Eqs. (7) and (13); and for this reason these results were again independently derived by following a different convention of rotations. Accordingly, taking the spin axis along the z axis, as depicted in Fig. 6 (in Fig. 5, x is the spin axis), both the horizontal and inclined axes results [Eqs. (13) and (7), respectively] could be verified.[7]

Aerodynamic Angles

Nonzero angles of sideslip are obtained by locking the model at a finite angle of roll ϕ_0 on the balance axis. In translational motion as well as in the mean condition during rotational motion, $\psi = 0$, and it can be shown that the aerodynamic angles of attack and sideslip $\hat{\alpha}$ and $\hat{\beta}$ are given by

$$\hat{\beta} = \sin^{-1}(\sin\alpha\sin\phi_0)$$

$$\hat{\alpha} = \tan^{-1}(\tan\alpha\cos\phi_0) \tag{21}$$

These relationships should be used in conjunction with Eqs. (3), (10), (15), and (19).

Low Frequency Restriction in Rotational Motion

The equations derived above for pure translational motion are exactly true for the complete model. On the other hand, in rotational motion the analysis is exact for motion at a point, nominally the center of mass, but a small velocity distribution is introduced as the direct consequence of the fact that Eq. (8) cannot simultaneously be satisfied at all points on the body.

To investigate the conditions under which the concomitant flow deviations may be neglected, consider the system with $\Lambda = \sigma$, where σ is not equal to $-\Omega$ but is nevertheless a small quantity. Then Eq. (13) yields the *local* velocity components

$$v = -V_\infty\sin\Phi(\Omega + \sigma)$$

$$w = V_\infty\sin\Gamma(1 - \sigma\Omega) + V_\infty\cos\Gamma\cos\Phi(\Omega + \sigma)$$

$$u = V_\infty\cos\Gamma(1 - \sigma\Omega) - V_\infty\sin\Gamma\cos\Phi(\Omega + \sigma) \tag{22}$$

If r_c is the orbital radius at an arbitrary point on the model axis, $\sigma = -\omega r_c/V_\infty$ and, neglecting terms of order Ω^2, the local angles of attack and sideslip and their derivatives may be expressed in the form

$$\beta_c = \sin^{-1}\{\sin\Phi(r_c/r_0 - 1)\Omega\}$$

$$\alpha_c = \tan^{-1}\left[\frac{\tan\Gamma - \cos\Phi(r_c/r_0 - 1)\Omega}{1 + \tan\Gamma\cos\Phi(r_c/r_0 - 1)\Omega}\right] \tag{23}$$

$$\dot{\beta}_c = \omega\Omega\cos\Phi(r_c/r_0 - 1)$$

$$\dot{\alpha}_c = \omega\Omega\sin\Phi(r_c/r_0 - 1) \tag{24}$$

To ensure that the curved flow effects may be ignored, it is necessary, firstly, that the deviation of the local aerodynamic angles on the model from their counterparts at the reference point, $\Delta\beta$, $\Delta\alpha$, should be smaller than the angular resolution of the data acquisition/reduction system. Then, expressing these deviations as fractions δ of the helix angle, it follows from Eq. (23) that

$$\Delta\beta, \Delta\alpha \leqq \delta\Omega \qquad r_c/r_0 - 1 \leqq \delta \tag{25}$$

Secondly, the derivatives of these local aerodynamic angles should not exceed a small fraction $\bar{\epsilon}$ of the corresponding body angular velocities. Equations (17) and (24) yield

$$\dot{\beta}_c \leqq \bar{\epsilon}r \qquad r_c/r_0 - 1 \leqq \bar{\epsilon}\cos\Gamma \tag{26a}$$

$$\dot{\alpha}_c \leqq \bar{\epsilon}q \qquad r_c/r_0 - 1 \leqq \bar{\epsilon} \tag{26b}$$

Since $r_c = r_0\{1 + (\omega x_c/V_\infty)^2\}^{1/2}$ and as the condition (26a) is more restrictive than (26b), the above conditions reduce to

$$\omega x_c/V_\infty \leqq (2\bar{\epsilon}\cos\Gamma)^{1/2} \text{ or } (2\delta)^{1/2} \tag{27}$$

Therefore, when the tangency condition is applied at $x_c = x_n/2$, where x_n is the nose coordinate, there is a frequency limit,

$$\Omega \leqq (r_0/x_n)(\delta\bar{\epsilon}\cos\Gamma)^{1/2} \text{ or } (r_0/x_n)(\delta\delta)^{1/2} \tag{28}$$

above which the curved flow effects may become significant.

Dynamic Stability Apparatus

The development of a dynamic stability apparatus incorporating the orbital fixed-plane principle is being considered at present.[7] A description of the mechanical details would be beyond the scope of this paper, but a brief discussion of the modes of operation is in order here.

Table 1 Modes of operation of an envisaged apparatus

Objective	Mode	Orbital axis	Typical α or β range, deg	Typical amplitude, deg	Non-zero adjustments	Continuous rotations
Dynamic derivative measurement	Fixed-plane translation	Horizontal	0-120	±2.5	r_0,Γ,ϕ_0	$\Psi=-\Phi$
		Inclined	0-40		r_0,Θ,ϕ_0	
	Fixed-plane rotation	Horizontal	0-120	±2.5	$r_0,\Lambda,\Gamma,\phi_0$	
		Inclined	0-40		$r_0,\Theta,\Lambda,\phi_0$	
	Lunar coning	Horizontal	0-120	...	Λ,Γ,ϕ_0	
Rolling		Inclined	0-40		Θ	Φ (Ψ = const)
Vehicle motion simulation	Oscillatory coning	Inclined	0-120	40	$\Theta,\Lambda,\Gamma,\phi_0$	
	Spinning			25	$r_0,\Theta,\Lambda,\Gamma,\phi_0$	
	Fixed-plane coning/ precession	Horizontal or inclined		±4	θ or Γ,Λ,ϕ_0	$\Psi=-\Phi$

It is planned to design the proposed apparatus such that it has the capability of testing 1/40-scale combat aircraft models at representative reduced angular velocities. As shown in Ref. 7, the frequency limit given by Eq. (28) is well above the proposed maximum orbital frequency of 40 Hz when $\bar{\epsilon}=0.1$. Moreover, it follows from Eq. (8) that at Mach 0.7 and 40 Hz an orbital radius of 24 mm (or around 18 mm for $\Theta=40$ deg) would yield an oscillatory amplitude of ±1.5 deg.

The prime purpose of the equipment is, of course, the determination of dynamic derivatives, but the ability to generate motions approximating aircraft modes is also considered important. The derivative measurement modes include the four fixed-plane modes described above, steady rolling, and lunar coning. The simulation modes include aircraft spinning, asymmetrical coning, and precessional motion (or fixed-plane coning). There are, therefore, nine distinct modes of operation, as summarized in Table 1. Other modes, such as wing rock, are feasible but will not be discussed here.

Dynamic Derivative Measurement Modes

Orbital Fixed-Plane Modes

Both the inclined and horizontal fixed-plane modes may be used to obtain linear acceleration and angular rate derivatives; in the former case the apparatus is inclined at an angle Θ (with $\Gamma=0$) and in the latter the pitch angle Γ is set on a knuckle aft of the balance ($\Theta=0$). The fixed-plane constraint $\Psi=-\Phi$ is implemented mechanically (see Table 1). Translational ($\Lambda=0$) and rotational ($\Lambda\neq 0$) motions are achieved with $r_0\neq 0$.

In rotational motion, these parameters are related to ω [Eq. (8)] and the position of the tilt axis is adjusted to maintain the location of the model center of mass relative to the platform frame of reference. The mean angles of attack and sideslip are determined by Θ, Γ, and ϕ_0.

Degenerate Modes

The characteristic, lunar coning motion may be generated by tilting the model through angles Γ and ϕ_0 with its center of mass on the orbital axis and $\Theta=\Lambda=r_0=0$. Note that, for small angles ($\Gamma\leqq 4$ deg), the same coning motion may be produced with $\Gamma\neq 0$ and $\Lambda=0$ and vice versa.

The angular velocities are

$$p=\omega\cos\Gamma$$

$$q=\omega\sin\Gamma\sin\phi_0$$

$$r=\omega\sin\Gamma\cos\phi_0 \tag{29}$$

In the steady rolling mode, $r_0=\Lambda=\Gamma=0$ and the motion parameters are

$$p=\omega$$

$$\dot{\alpha}=\frac{-\omega\sin\Phi\tan\theta}{1+\cos^2\Phi\tan^2\Theta}$$

$$\dot{\beta}=\omega\cos\Phi\sin\Theta\,(1-\sin^2\Phi\sin^2\Theta)^{-1/2} \tag{30}$$

The coning and rolling modes are degenerate fixed-plane motions since they involve only one axis of continuous rotation.

Approximate Simulation of Vehicle Motion

Oscillatory Coning and Spinning

The conditions for oscillatory coning are the same as for lunar coning, except that here Θ is non-zero. Steady spinning is the most general case of asymmetrical coning, involving a finite spin radius. The fixed adjustments include $r_0\neq 0$ and/or $\Gamma>-\Lambda\gg 0$.

Fixed-Plane Coning/Precession

The model axis is tilted radially with $r_0=0$. Various types of coning or precessional motions result, depending on the pivotal angles Θ, Λ, and Γ. For instance, when $\Theta=\Gamma=0$, oscillatory pitching and yawing and steady coning at small amplitude is obtained. On the other hand, when the model and orbital axes are tilted in opposing directions ($\Theta>0$ and $\Gamma<0$), small-amplitude, high $-\alpha$ precessions may be generated.

Aerodynamic Testing Considerations

Typical incidence and amplitude ranges are given in Table 1, representing nominal limits for subsonic tests in the NAE 30-in. wind tunnel. In principle, the orbital fixed-plane testing concept is also applicable in high-Reynolds-number transonic and supersonic tunnels. Several optional sting arrangements are contemplated to facilitate tests of configurations which cannot be conventionally sting mounted, e.g., models with boattails or twin tailpipes.

The question of sting interference was discussed in Ref. 7 and only a few remarks will be made here. Dynamic sting interference is expected to be small in most experiments since there is virtually no lateral motion of the model relative to the sting in the vicinity of the model base. Moreover, there are no significant sting oscillations due to static aerodynamic forces in the case of well-adjusted fixed-plane rotational motion since the angles of attack and sideslip are invariant [Eqs. (15) and (21)] or effectively constant [Eqs. (10) and (21)].

Data Acquisition and Reduction

The salient difference between this and conventional data reduction procedures arises in that the primary motion is forced in 2DOF instead of one. Reactions will therefore be induced in the DOFs which convey the primary motions as well as in the secondary DOFs. This situation presents no real difficulty for reasons discussed below.

Data Acquisition Procedure

In general, the loads sensed by the five-component balance comprise inertial, gravitational, and aerodynamic static and dynamic loads on the model. All of the induced reactions are sinusoidal and synchronous with the orbital motion and may be separated if the following tests are performed for identical values of the model position parameters.

1) Static tare: In this experiment the model is orbited *slowly* in the presence of wind-tunnel flow at the prescribed Mach number. Dynamic effects may be neglected and the reactions are due to static aerodynamics and inertial and gravitational effects only.

2) Slow tare: The model is again orbited at the same frequency as in test 1, but in the absence of flow. The concomitant reactions are due to inertial and gravitational effects only and equal to their counterparts in test 1. The desired static loads may therefore be obtained by subtracting the deflection vectors recorded in test 2 from those in 1. Although the static reactions due to both primary DOFs are present, they are separable by virtue of the fact that the primary motions are known in terms of the orbital angle Φ, and in phase quadrature, a relationship that is preserved amongst the reactions.

3) Dynamic test: In the actual dynamic test the model is orbited at the prescribed frequency in the presence of flow at the set conditions. The reactions measured now comprise the dynamic and static aerodynamics as well as inertial and gravitational contributions.

4) Fast tare: Finally, the model is orbited at the prescribed frequency as in test 3 but in the absence of flow. Therefore, the measured reactions are purely inertial and gravitational and equal to their counterparts in 3.

A vectorial subtraction of the appropriate quantities obtained in tests 3 and 4 yields the combined aerodynamic static and dynamic components. The static components extracted in 2 can then be subtracted and the remaining dynamic components may be separated as they are in phase quadrature.

The slow tare is not strictly essential but is designed to enhance the data acquisition process and might be omitted under favorable experimental conditions. Also, in certain cases, the slow tare would be rendered superfluous by the nature of the motion analyzed[7] (as in translation). In other circumstances, for instance, in the rotational modes, the static tare may be eliminated.[7]

Data Reduction

The data reduction procedure for the determination of cross-coupling derivatives involves the extraction of in-phase and quadrature components of the loads producing the secondary DOF deflections through a cross-correlation process. These methods have been well documented[9] and will not be discussed here.

The reference signal required for correlation purposes can be generated by means of a position encoder. It is necessary to know the functional nature of the motions in the secondary DOFs a priori if the effects submerged in the corresponding signals are to be extracted. The primary motions are effectively sinusoidal at all amplitudes considered so that the responses in the secondary DOFs must also be sinusoidal. This does not involve any assumption of linearity as required in an elastic system since the form of the signals is given by their relationships to the reference signal.

Parameters of the Primary Motion

Considering the individual primary motions, it may be observed that the amplitude of the oscillations is essentially equivalent to that found in existing pitch-yaw apparatuses.[1,3] On the other hand, results have been obtained at effective amplitudes of only ± 0.1 deg in translational experiments.[2] Since the angular displacements of the translational and rotational fixed-plane modes are the same, typically ± 1.5 deg at Mach 0.7 and 40 Hz, the new apparatus could yield amplitudes one order of magnitude larger.

In contrast to conventional forced-oscillation methods, the orbital fixed-plane principle has the advantage of explicitly known relationships between the rotational and translational components. These rates, as well as the position and

Table 2 Dynamic stability derivative matrix

Mode	Parameter[a] $\dot{\alpha}$	$\dot{\beta}$	p	q	r	Derivative, $i=Y,Z,l,m,n$
Translation						
Horizontal	A	B	0	0	0	$C_{i_{\dot{\beta}}}, C_{i_{\dot{\alpha}}}$
Inclined	$\frac{A\cos\Theta}{\Delta}$	$\frac{B}{\Delta^{1/2}}$	0	0	0	
Rotation						
Horizontal	0	0	$-B\sin\Gamma$	$-A$	$B\cos\Gamma$	C_{i_q}, C_{i_r}
Inclined	$\frac{-A\sin^2\Theta}{\Delta\cos\Theta}$	0	0	$\frac{-A}{\cos\Theta}$	$\frac{B}{\cos\Theta}$	
Coning	0	0	Π	$P\sin\phi_0$	$P\cos\phi_0$	$C_{i_{\dot{\lambda}}}$

[a] $A=-\omega\Omega\sin\Phi$; $B=-\omega\Omega\cos\Phi$; $\Delta=1+2\Omega\cos\Phi\sin\Theta$; $\Pi=\omega\cos\Gamma$; $P=\omega\sin\Gamma$.

aerodynamic angles, are analytical functions of a single time-dependent variable Φ. The motion frequency ω and the amplitudes of the motion are effectively constant, by virtue of the inexorable characteristics of the drive system.

The parametric relationships are summarized in Table 2 for the different modes of operation. The oscillations generated are all either pure sinusoids, or effectively sinusoidal, and in some cases, e.g., translational motion, uncontaminated by fluctuations in other parameters. The residual $\dot{\alpha}$ and p terms associated with the rotational modes are fortunately small and accountable.

Dynamic Stability Derivatives

Since the apparatus can operate in translational, rotational, coning, and rolling modes, it is capable, in principle, of yielding all of the first-order dynamic stability derivatives, including those due to $\dot{\beta}$, $\dot{\alpha}$, p, q, r, and $\dot{\gamma}$.

The aerodynamic derivatives summarized in Table 2 are expressed in the body axes system. The set C_{i_q}, $C_{i_{\dot{\alpha}}}$, C_{i_r}, $C_{i_{\dot{\beta}}}$, $C_{i_{\dot{\chi}}}$ constitutes a complete set of derivatives in the formulation of Tobak and Schiff[8] for an aircraft undergoing slowly varying motions where the swerving is small. In the case of an axisymmetrical body C_{i_p} may be determined in the steady rolling mode in addition to the Magnus moment coefficient. Then a complete set of derivatives expressed in the aerodynamic axes system comprises C_{i_p}, $C_{i_{\dot{\delta}}}$, and $C_{i_{\dot{\chi}}}$, where δ is the resultant angle of attack.

Hence, in principle, the orbital apparatus is capable of determining two different, complete sets of dynamic data compatible with the Tobak-Schiff model. However, the set of motions from which they are derived are not identical to those prescribed by the model, as will be discussed later. This facility for determining all of the derivatives by means of a single apparatus is certainly a valuable one; the potential advantages of consistency and saving in effort are considerable.

Sources of Uncertainty

As in any complex technique, the advantages of the present approach are not undiluted and an effort is made to identify the major sources of uncertainty.

First of all, there is the category of errors which can, in principle, be accounted for. When the effects due to small motion impurities present in the rotational (see Table 2) and rolling modes are considered significant (i.e., at large Θ or Γ), they may be eliminated by interrelating the results with data from complementary tests. The spurious $\dot{\alpha}$ effect present in the rotational modes [Eq. (24)] is not a concern, since its frequency threshold is beyond the design maximum for the proposed apparatus. Other, similar effects due to radial sting deflection may be eliminated through an angular offset correction.

In translational fixed-plane motion the static derivatives are in-phase with their out-of-plane dynamic counterparts so that these derivatives will in fact be determined in the combinations $C_{i_{\dot{\beta}}} + C_{i_\alpha}$ and $C_{i_{\dot{\alpha}}} + C_{i_\beta}$, assuming that the higher-order derivatives $C_{i_{\dot{\beta}}}$ and $C_{i_{\dot{\alpha}}}$ are negligible. Although C_{i_α} and C_{i_β} may be accounted for in the tare test procedure, this remains a potential source of uncertainty.

The basic oscillatory loads of the model at the balance center, on the other hand, constitute a source of error which cannot be eliminated. Although extracted in a fast tare test, the inertial deflection vector is otherwise indistinguishable from its aerodynamic counterpart, and clouded by noise. These configuration-dependent effects could greatly affect the accuracy, but may be minimized by appropriate model design. Moreover, any center-of-mass offset with respect to the reference center on the sting axis could degrade the accuracy for the same reason, but may be eliminated completely through correct model mounting.

Also in the category of errors about which little can be done is the uncertainty due to the presence of higher-order rotational derivatives. If the second-order derivatives are significant, then the rotational combinations determined will be $C_{i_{\dot{r}}} + C_{i_q}$ and $C_{i_{\dot{q}}} + C_{i_r}$ and additional tests will be required to estimate the $\dot{q}$ and $\dot{r}$ derivatives.

Finally, there is the problem of corotation of air due to the motion of the model and sting. It would be difficult to estimate the effects of swirling on derivatives and it will suffice to emphasize that they deserve serious attention, as is indeed the case in all rotary wind tunnel experiments.

Applications in Flight Mechanics

The potential applications of the concepts introduced are considered here with a view to expanding the experimental basis of flight mechanics. Two sources of preoccupation of the flight dynamicist are pertinent to this discussion, viz., the validity of mathematical models of the aerodynamics of the aircraft and the extent to which the derivatives formulated in these models are influenced by experimental conditions.

Mathematical Modeling

Traditionally, the model prescribes a series of 1DOF characteristic motions for which the aerodynamic reactions are to be measured. While the purpose is to relate these responses to the aircraft motion in flight, there is a contradiction when high angles of attack or rotation rates are involved. The reactions to the characteristic motions cannot simply be superimposed when separated flow conditions prevail, since such a premise implicitly assumes that the associated flowfields may be superimposed to yield the complex flowfield of the free motion.

Cognizant of these shortcomings, the orbital motion concept was introduced with a view to obtaining comprehensive, nonplanar-motion-dependent aerodynamics. Of course, this suggests the possibility of a new nonlinear mathematical model. However, its formulation is beyond the scope of the present discussion, which is concerned with the introduction of new dynamic testing concepts within the framework of the existing mathematical model.[8]

The Tobak-Schiff model specifies the following characteristic motions in body axes: steady planar motion at fixed attitude, planar pitching oscillations, yawing oscillations, and steady coning.[8] The coning mode of the orbital apparatus is as prescribed, while the pitching and yawing oscillations are equivalent to their planar counterparts if it may be assumed that only linear effects are present.

When this premise fails, a means must be found to identify nonlinearities due to the nonplanar motion shape. To identify the second-order effects, the first-order derivatives might be correlated with the frequency ratios $\dot{\beta}/\dot{\alpha}$ and r/q, and some parameter dependent on the motion shape, for instance, describing the motion eccentricity, ϵ_α and ϵ_θ,

$$\epsilon_\alpha = (\beta_{\max} - \beta_{\min})/(\alpha_{\max} - \alpha_{\min})$$

$$\epsilon_\theta = (\psi_{\max} - \psi_{\min})/(\theta_{\max} - \theta_{\min}) \qquad (31)$$

where $\beta_{\max}$ and $\beta_{\min}$, etc., are the maximum and minimum absolute values. Finally, a nonlinear model would be devised to correctly synthesize the first- and second-order responses determined (see also Ref. 7).

The purpose is not to pursue this point but to illustrate how the capability of extracting derivatives for different combinations of the motion variables might be exploited. Different ratios of $\dot{\beta}$ and $\dot{\alpha}$ can be obtained at otherwise identical conditions by testing in both inclined and horizontal modes [Eqs. (4) and (20)]. The total lateral acceleration $(\dot{\alpha}^2 + \dot{\beta}^2)^{1/2}$ can be kept constant in the two cases using appropriate settings of the respective orbital radii. On the other hand, the acceleration and rotational derivatives may be determined for identical magnitudes of $\dot{\alpha}$, $\dot{\beta}$ and q, r, respectively.

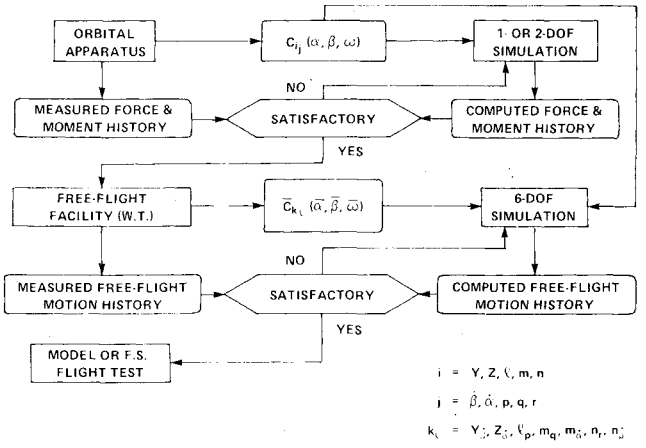

Fig. 7 Data/model validation scheme.

Data/Model Validation

The validation of the aircraft mathematical model and the aerodynamic data is best achieved through correlation of free-flight and simulated data.[4] However, since such a validation process is not a simple matter, it is desirable to perform other checks at intermediate stages of the production of the aerodynamic data. Hence it could be most advantageous if the validity of dynamic wind tunnel data per se could be confirmed by means of another wind tunnel experiment. This becomes feasible if an intermediate motion simulation can be generated by the same apparatus used to obtain the derivatives in the first place, since then the effects of interference, instrumentation errors, and facility deviations (e.g., flow nonuniformity) will be consistent.

The first step would be to compare the orbital derivative data with their counterparts in conventional forced-oscillation tests. The latter are the derivatives for nonfinite ϵ_α and ϵ_θ [Eq. (31)]. The results of this comparison could indicate specific mathematical modeling requirements (see above).

The nature of the intermediate validation scheme proposed is explained with reference to Fig. 7. The aircraft motion of interest, for instance, a steady spin, is simulated mechanically on the orbital apparatus to obtain a motion having only one independent DOF, but nevertheless approximating the aircraft mode in flight. It is important to note that this simulation *does not predict* actual flight since the 1DOF motion constraint inhibits the flowfield about the model. Force and moment histories are recorded during this motion and compared with a numerical simulation similarly constrained to 1DOF and utilizing the dynamic derivatives previously determined on the same apparatus. If the agreement is found unsatisfactory, the aerodynamic force model is modified, for instance, by adjusting the nonlinear terms and the process repeated. A satisfactory match will at once provide confidence in the model as well as in the dynamic data utilized. When this has been achieved, the validation process may be taken a step further with analogous comparisons of free-flight and computational simulations, in this case matching the motion histories.

In this way, the problem of handling the complexity of arbitrary 6DOF, high-α motion is approached by dissection into several steps, each of which involves the lowest possible level of uncertainty and a minimum of assumptions. The method is equally applicable to the various modes of aircraft motion, including spinning, wing rock, snaking, and precession.

Combinations of Characteristic Motions

The fact that the pitching and yawing oscillations are keyed together in the basic motion for the determination of rotational derivatives is no disadvantage and is, in fact, analogous to the situation in coning, where the pitching, yawing, and rolling oscillations are locked together. This is also true of the translational mode, and any captive testing method involving a single independent DOF.

On the other hand, as far as actual aircraft motions are concerned, the constraint of 1DOF is a disadvantage which rules out any direct simulations. This is equally true of the simulation of spinning on a rotary rig or lateral oscillations by means of fixed-plane coning. However, it is no drawback in the validation scheme discussed above, where the "simulations" only represent one step in a procedure designed to bridge the gap between wind tunnel results and full-scale predictions.

More specifically, composite motions provide opportunities to check the superposition principle implicit in the mathematical model. For instance, the fixed-plane coning mode may be applied to check the equivalence of aerodynamic response constructed from the individual responses to pitching oscillations, yawing oscillations, and steady coning and that due to simultaneous pitching and yawing with steady coning.

Conclusion

A new approach to dynamic stability testing has been introduced, based on the concept of orbital fixed-plane motion. An apparatus implementing this concept could, in principle, be used to yield all of the important direct, cross, and cross-coupling dynamic stability derivatives. The device could be operated in several different modes facilitating the determination of linear-acceleration, rotational, and coning derivatives on the one hand, and the approximate simulation of flight vehicle motions (such as aircraft spinning and other high-α behavior) by means of combinations of characteristic motions, on the other.

The greatest benefit to be derived from the capability of generating representative motions on the same apparatus used for derivative measurements is the opportunity to directly enhance the credibility of the aerodynamic data and mathematical models employed in predictions of flight vehicle behavior. Accordingly, an aerodynamic data/model validation scheme has been presented for the exploitation of this facility.

The new techniques should be developed in conjunction with conventional forced-oscillation experiments, since the latter provide the planar counterparts of the nonplanar primary motion relationships. The concepts are seen to be applicable to high-Reynolds-number testing at subsonic, transonic, or supersonic Mach numbers. Moreover, dynamic sting interference and sting oscillations can be significantly reduced in certain modes of orbital motion, particularly in the pure-rotation mode.

The set of dynamic derivatives will be determined for explicitly known motion conditions, with an inherent flexibility which permits changing the relationships between the motion variables in the two primary degrees of freedom. It is thought that this capability, used in concert with the facility for producing combinations of characteristic motions, could contribute to the verification of the existing aircraft mathematical models and facilitate future modeling efforts.

References

[1] Orlik-Rückemann, K.J., "Review of Techniques for Determination of Dynamic Stability Parameters in Wind Tunnels," AGARD LS-114, Paper 3, March 1981.

[2] Orlik-Rückemann, K.J., "Wind Tunnel Apparatus for Translational Oscillation Experiments," AIAA Paper 80-0046, Pasadena, Calif., Jan. 1980.

[3] Hanff, E.S. and Orlik-Rückemann, K.J., "A Generalized Technique for Measuring Cross-Coupling Derivatives in Wind Tunnels," AGARD CP-235, Paper 9, May 1978.

[4] Beyers, M.E., "Investigation of High-Manoeuvrability Flight Vehicle Dynamics," *Proceedings of the 12th ICAS Congress*, Paper 7.2, Oct. 1980, pp. 278-292.

[5]Malcolm, G.N., "Rotary and Magnus Balances," AGARD LS-114, Paper 6, March 1981.
[6]Orlik-Rückemann, K.J., "Dynamic Stability Testing in Wind Tunnels," NAE LTR-UA-41, Ottawa, March 1977.
[7]Beyers, M.E., "A New Concept for Dynamic Stability Testing," NAE LTR-UA-53, Ottawa, Canada, Sept. 1980; see also, AIAA Paper 81-0158, Jan. 1981.
[8]Tobak, M. and Schiff, L.B., "On the Formulation of the Aerodynamic Characteristics in Aircraft Dynamics," NASA TR R-456, Jan. 1976.
[9]Hanff, E.S. and Orlik-Rückemann, K.J., "Wind Tunnel Determination of Dynamic Cross-Coupling Derivatives—A New Approach," *Israel Journal of Technology*, Vol. 18, No. 1, 1980, pp. 3-12.